BILINGUAL PUBLISHING GROUP

Southeast Asia Development Research

https://journals.bilpubgroup.com/index.php/sadr

ARTICLE

Palm, Rubber and Rice Crops Classification and Diagnostic Using CNN Approach and NDVI in Thailand

Yannis. Lavigne [1], ***Laurent. Mezeix*** [2 *]

[1]*INSA Toulouse, Toulouse Cedex 31077, France*

[2]*Faculty of Engineering, Department of Advanced Materials Engineering, Burapha University, Chonburi 20131, Thailand*

ABSTRACT

To support agricultural development in Thailand, accurate data collection and analysis of land use are essential. Understanding the spatial distribution and growth patterns of key crops enables better planning and resource allocation. This study proposes a deep learning-based approach for land cover classification, specifically targeting three significant crops: rice, rubber, and palm. A Convolutional Neural Network (CNN) is employed to classify satellite imagery into these three categories. The datasets used in this research are derived from high-resolution Pleiades satellite imagery and consist of three independent datasets, each containing 200,000 image tiles of 100x100 pixels. For each crop type, a dedicated CNN model are trained and optimized, achieving classification accuracies exceeding 90%. After prediction, a post-processing step is implemented to merge tile-level classifications into continuous land cover maps. This enables a clearer spatial visualization of crop distribution. Furthermore, a clustering algorithm is applied to identify individual agricultural fields, which facilitates further analysis. Vegetation health and maturity are assessed using the Normalized Difference Vegetation Index (NDVI), from which the approximate age of the crops is inferred. These parameters are then used to estimate the potential agricultural yield or production for each field. To validate the approach, a large area of 100 square kilometers is analyzed, and the model's classification results are compared against manually labeled reference data provided by the Thailand Space Agency. The comparison reveals a classification discrepancy of -12% for palm crops and approximately -20% for both rice and rubber, demonstrating the model's high potential for scalable crop monitoring.

Keywords: Convolutional Neural Network (CNN); Image Processing; Land Cover; Satellite Image; NDVI

*CORRESPONDING AUTHOR:

Laurent Mezeix, Faculty of Engineering, Department of Advanced Materials Engineering, Burapha University, Chonburi 20131, Thailand;
Email: laurentm@eng.buu.ac.th

ARTICLE INFO

Received: 11 January 2025 | Revised: 19 February 2025 | Accepted: 26 February 2025 | Published Online: 10 March 2025
DOI: https://doi.org/10.30564/sadr.v1i1.9564

CITATION

Lavigne, Y., Mezeix, L., 2025. Palm, Rubber and Rice Crops Classification and Diagnostic Using CNN Approach and NDVI in Thailand. Southeast Asia Development Research. 1(1): 31–46. DOI: https://doi.org/10.30564/sadr.v1i1.9564

1. Introduction

According to the United Nations, the global population is estimated to reach 8.5 billion by 2030 and 9.7 billion by 2050. In this context, ensuring food security has become a critical challenge, requiring an increase in global food production [1]. Effective monitoring of agricultural land and production management plays a crucial role in addressing this issue [2]. However, boosting productivity without depleting finite resources remains a major challenge for agriculture. Precision agriculture, which leverages digital technologies such as remote sensing, offers a promising solution by optimizing agricultural performance [3].

Recent advances in remote sensing technologies—deployed via satellites, aircraft, or drones—enable efficient monitoring and detection of land characteristics [4]. The growing accessibility of land cover data has further expanded their applications [5]. In Thailand, for instance, these technologies have been widely utilized to study the evolution of crop types [6], map aquaculture zones [7], and conduct hydrological analyses [8]. Traditional mapping approaches often rely on multi-temporal observations and are primarily based on statistical models or index-based methods [9–12]. However, these methods may struggle to capture complex spatial patterns, particularly in heterogeneous landscapes, leading to misclassifications or inaccuracies [13].

CNNs have become a dominant approach in land classification due to their superior performance compared to traditional machine learning methods such as Support Vector Machines (SVM), Random Forest (RF), and logistic regression [14–17]. Studies demonstrate that CNNs achieve higher accuracy in various applications, including a 12% improvement over SVM in groundwater potential mapping [16] and better performance in assessing water quality in Brazil's Tietê River [14]. Beyond land classification, CNNs have significantly advanced agricultural management by automating tasks traditionally performed manually, reducing costs, and improving efficiency. Their applications include plant and weed recognition [18, 19], as well as tree counting for plantation monitoring [20].

For instance, oil palm tree detection—a critical task for plantation management—often relies on LeNet-based CNN architectures trained on high-resolution QuickBird imagery (0.3–2.4 m). These models, trained on datasets ranging from 3,000 to 19,000 image tiles, consistently achieve an accuracy of over 94% [21]. Similarly, in rice field monitoring—a priority for Asian food security—CNNs face challenges due to phenological variations across growth stages (tillering, heading, and harvest). An Recurrent Neural Networks (RNN) based study in West Java achieved 75% accuracy using 130,000 images spanning three growth stages [22]. In contrast, Enhanced-TransUnet (ETUnet), applied to drone imagery, classified combined stages with an F1-score of 94%, although individual stage detection dropped to 50–70% [23]. Another approach, FR-Net, trained on 31,909 Landsat 8 tiles (256 × 256 pixels), achieved 88.4% accuracy but required high-performance Graphics Processing Units (GPUs), thereby increasing computational costs [24].

To further enhance accuracy, CNNs can integrate multispectral data or physical models [25]. Vegetation indices, for example, are often combined with CNN outputs to improve assessments of crop health and density, demonstrating the flexibility of these methods in precision agriculture.

Vegetation indices are numerical measures derived from remote sensing data, typically satellite imagery [26]. These indices are valuable tools used in various fields, including agriculture, forestry, environmental monitoring, and land management. They provide useful insights into vegetation dynamics and can be used to study changes in vegetation over time and space. The fundamental principle behind vegetation indices is that plants reflect and absorb different wavelengths of light [27]. In particular, they strongly absorb visible light for photosynthesis while reflecting a significant amount of near-infrared (NIR) light. Vegetation indices utilize these characteristics to calculate ratios or combinations of spectral bands from the remote sensing data to infer vegetation properties. One of the most well-known and widely used vegetation indices is the Normalized Difference Vegetation Index (NDVI) [28]. NDVI has allowed for wide application in vegetative studies, as it is used to estimate crop yields (Peters et al., 2002) and the age and productivity of rice [29], palm age and nutrient deficiencies [30] or rubber stand age [31]. The relationship between NDVI and crop age stems from the predictable changes in canopy reflectance during plant development. Young crops exhibit low NDVI values during establish-

ment, which increase sharply during vegetative growth as the leaf area expands, and then gradually decline during maturation and senescence. By tracking these NDVI patterns against known phenological curves, crop age can be estimated with reasonable accuracy, especially when calibrated with ground-truth growth stage data.

This paper aims to develop a tool for performing land cover classification of agricultural fields and to propose a diagnostic assessment of crop age and production using external data. The tool is designed to support Thailand's space agency, Geo-Informatics and Space Technology Development Agency (GISTDA) in providing accurate agricultural information to the Thai Ministry of Agriculture. A case study demonstrates the tool's effectiveness by classifying three crop types: rice, palm, and rubber. To achieve this, CNNs are employed for classification, with four distinct classes established: rice, palm, rubber, and a complementary class. These classes are used to generate three datasets. The methodology for analyzing rice, rubber, and palm fields is detailed, and CNN models tailored to each dataset are proposed and validated. The land cover classification is first evaluated on a small test area, followed by a large-scale assessment and diagnostic analysis of a 100 km² region using NDVI data.

2. Methods

2.1. Land Cover

The method for generating the land cover by combining the results from different CNNs is briefly outlined, and readers are referred to the following publication for further details [32]. Each CNN model is used to predict a specific class, and then, post-processing is performed on each classification to remove classified spots that are too small to actually represent the feature they are intended to represent. Finally, the land cover is performed by assembling the different class prediction results.

2.2. Crops Diagnostic

The CNN-based classification provides detailed crop information, including crop type (class), area (size), and spatial distribution (location). By integrating this data with external sources, it becomes possible to derive/extract comprehensive agricultural insights. To facilitate this process, an eight-step methodology is proposed (**Figure 1**).

a) A remote-sensing image is used as input to the method (**Figure 1a**). For each investigated class, the CNN models classify the input images. Since the clustering approach based on the K-means method demonstrated its effectiveness in grouping predictions [25, 32], it is used to identify class-specific spots and determine their size and position (**Figure 1b**).

c) Index map is obtained from the index calculation, such as NDVI, Soil Adjusted Vegetation Index (SAVI), or Modified Green Red Vegetation Index (MGRVI), that are related to the remote sensing image bands as Red, Green, Blue Near Infrared bands also called RBG-NIR (**Figure 1c**). These indices are used to calculate a large number of vegetation parameters, including canopy health, biomass, and photosynthetic activity.

d) The index values, derived from the index map (**Figure 1c**), are assigned to each sampling point within their respective vegetation class (**Figure 1d**). This association enables the analysis of spatial variability in vegetation health and productivity across different classified zones.

e) The distribution of index values across all sampling points is analyzed (**Figure 1e**), providing statistical insights into vegetation variability within and between classes.

f) The class state (e.g., maturity stage or age) is correlated with a defined range of index values, as supported by external data from literature or field measurements (**Figure 1f**). This establishes a reference framework for interpreting vegetation conditions.

g) Using the class state information (**Figure 1f**) and the index distribution of each sampling point (**Figure 1d**), sub-classification based on developmental stages (e.g., young, mature, senescent) is performed. All relevant data per spot—including index values, class, and sub-class—are then systematically compiled (**Figure 1g**).

h) To enhance accessibility and utility for decision-makers, the aggregated data is organized into a structured format (e.g., geodatabase, tabulated reports, or interactive maps) tailored to stakeholder needs (**Figure 1h**).

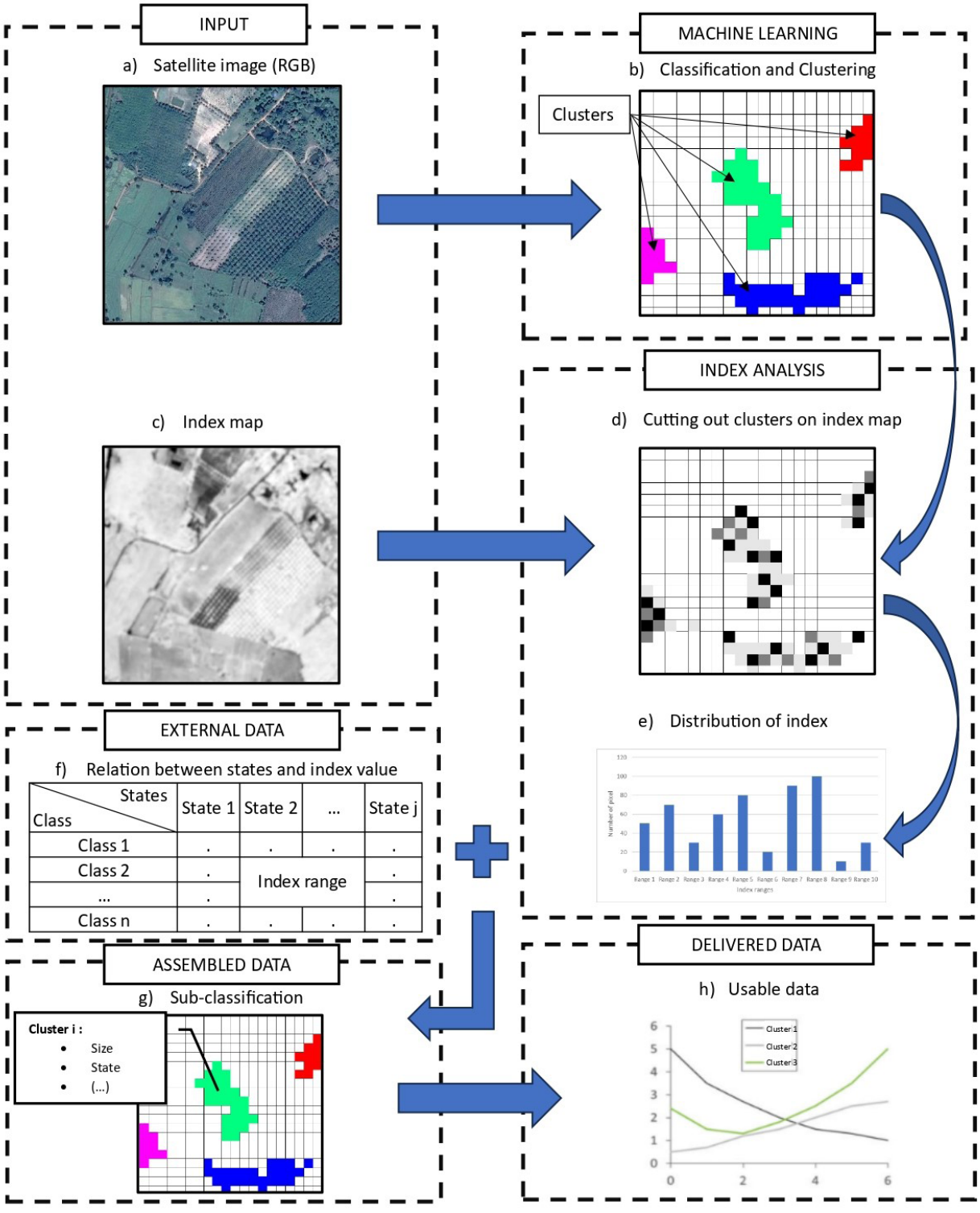

Figure 1. Methodology to perform diagnostics for each crop type.

3. Study Case

3.1. Interest

Thailand encompasses a total area of 513,000 km², with agricultural land covering 221,000 km² (43% of the national territory) as of 2015. The agricultural sector plays a vital role in Thailand's economy, contributing 8.7% to the Gross Domestic Product (GDP) and employing one-third of the nation's workforce in 2019. Thailand ranks among the world's leading producers of rice, rubber, and oil palm. Notably, it is the second-largest rice exporter globally, trailing only China, India, Indonesia, Bangladesh, and Vietnam in total production [33]. Moreover, Thailand accounts for 4% of the global palm oil production [34]. As of 2021, Thailand remains the global leader in natural rubber production, yielding 4.6 million metric tons annually. This accounts for approximately 35% of global rubber production, maintaining the country's dominant position in this agricultural sector since 1991 [35].

3.2. Dataset

To classify the three target agricultural types in Thailand (rice, palm, and rubber), we established four distinct classes:

- Rice class
- Palm class
- Rubber class
- Complementary class: Includes roads, buildings, non-target crops, and forests

The first three classes correspond to their respective crop types, while the complementary class encompasses all other land cover features (**Figure 2**). The dataset was derived from Pleiades satellite imagery (RGB bands, 0.5 m/pixel resolution) acquired on November 2, 2022. The study area comprises two 100 km² sites in Chachoengsao, Thailand, centered at: 13°39'9.171"N, 101°36'21.846"E; 13°20'20"N, 101°38'24"E. Each image tile measures 100 × 100 pixels (0.025 km² per tile). To ensure classification accuracy exceeding 90%, we followed established best practices [32, 36–39], requiring hundreds of thousands of high-quality tiles per class. Accordingly, our dataset includes 100,000 tiles per class for robust model training.

The three investigated classes (rice, palm and rubber) are identified by a specific CNN model, and therefore, three datasets must be organized using the same initial tiles. Each dataset is built around two subclasses (**Table 1**): the first class is the investigated one, and the second is referred to as 'others'. This second subclass is a combination of approximately 33,300 tiles from the three other non-investigated classes. As recommended in the literature, the dataset has been randomly divided into three sets: 70% of the total tiles as a training set, 15% as a validation set, and 15% as a testing set [40].

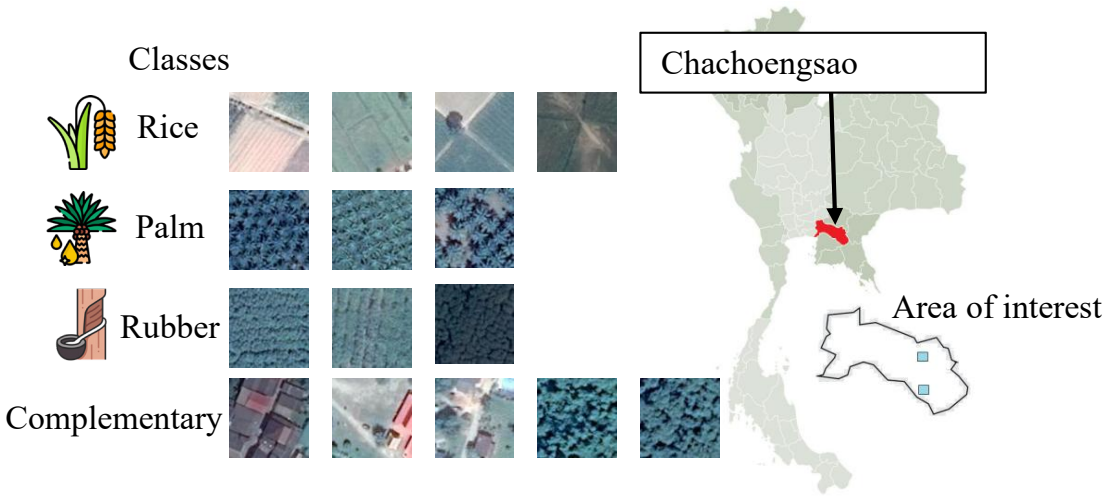

Figure 2. Typical class tiles are used to perform the classification and geographic location of the study area.

Table 1. Dataset.

	Dataset	
	sub-class 1: investigated class	sub-class 2: others
CNN model Rice	Rice class = 100,000 tiles	Rubber + Palm + complementary classes = 100,000 tiles
CNN model Rubber	Rubber class = 100,000 tiles	Rice+ Palm + complementary classes = 100,000 tiles
CNN model Palm oil	Palm oil class = 100,000 tiles	Rice + Rubber + complementary classes = 100,000 tiles

3.3. Land Cover

In the investigated study case, using the specified resolution, the parameters of the land cover post-processing have been empirically determined based on the experience of the GISTDA(**Table 2**).

Table 2. Post-processing of land cover.

Threshold \ Class Model	Rice	Palm	Rubber
Small size threshold main class cluster (m²)	600	2500	2500

3.4. Vegetation Indices

NDVI is an index commonly used in remote sensing and satellite imagery analysis to assess and quantify the amount of live green vegetation in a given area [41]. NDVI analysis is further used as ancillary data to support classification, resulting in differentiating between different types of vegetation, namely rice, forest, oil palm, matured rubber, and immature rubber classes, specifically [42]. The NDVI value was calculated using **Equation (1).**

$$NDVI = \frac{NIR - RED}{NIR + RED} \quad (1)$$

Where Red and NIR are the Band 3 (620-700 nm) and the Band 4 (775-915 nm) respectively in Pleiade ("Pleiades - Earth Online," n.d.). Thanks to the land cover obtained using the aggregation of CNN models' results (**Figure 1b**) and the NDVI map (**Figure 1c**), index analysis can be performed (**Figures 1d** and **1e**). Based on external data, i.e. literature, NDVI values enable the determination of the age of rice, palm and rubber fields (**Figure 1f**). Then, information related to each field is collated (**Figure 1g**) and gathered (**Figure 1h**). Subsequently, a map displaying the age of fields is generated.

3.5. Rice Field

Using the NDVI, the age of rice can be determined [29], which is then utilized to estimate rice productivity [43]. The NDVI value utilized corresponds to the optimal vegetative phase of rice, occurring between 8 and 13 weeks after planting [44]. **Table 3** presents the NDVI classification table used to identify the age of rice. As given by the Equation 2, a typical rice field produces an average of 2300 kg/ha in Thailand [45].

$$\text{Average production(kg)} = 2300(\text{kg/ha}) \times \textit{area}(\text{ha}) \quad (2)$$

Table 3. Range of NDVI values for the ages of rice [29].

States	Age (weeks)	NDVI
Flooding	<3	<0.17
Tilering	3-<4	0.17-0.31
Stem Elongation	4-6	0.31-0.45
Panicle Initiation	6-8	0.45-0.52
Flowering	8-13	0.52-0.88
Fully-Mature	13-16	0.45-0.52
Harvesting	>16	0.31-0.45

3.6. Palm Field

Palms go through different stages of development: seed, young, teen and mature, and for each of them, palm oil production can be estimated [46]. Palm production is based on a 6-month period, which is the maturation time. As for the rice, the age of the palm trees can be obtained thanks to the NDVI [29]. The relation between age and NDVI is given by the following regression **Equation (3)**.

$$NDVI = 0.0104x + 0.5953 \quad (3)$$

Where x is the palm tree age.

Table 4. Production for each palm class and per age [46].

States	Seed	Young	Teen	Mature
Age (years)	0-3	3-8	9-14	15-25
NDVI	0.595-0.626	0.626-0.678	0.689-0.740	0.751-0.855
Average production (kg/6 months/ tree)	0	68.77	109.08	73.91

The canopy area of individual palm trees can be obtained from their age [47] and it is obtained using Equation (4), which is derived from field-measured crowns.

$$\text{Canopy area} = \frac{Age - 0.59}{0.15} \quad (4)$$

Finally, the total production can be calculated using the following **Equation (5)**.

$$\text{Total production} = \sum_{i=1}^{4}, \quad (Prod_i \text{ x } Number\ of\ palm\_tree_i) \quad (5)$$

Where '$Prod_i$' is the production of palm trees depending on their age (**Table 4**). 'Number of $palm\_tree_i$' is the estimated number of palm trees per age that is given by the total area divided by the canopy area of an individual palm tree [**Equation (4)**].

3.7. Para-Rubber Field

The development stages of a para-rubber plantation can vary slightly depending on specific management practices and regional factors such as climate, soil quality, agricultural practices, disease control, and the use of improved rubber tree varieties. However, here are the typical four development stages of a para-rubber plantation [48]:

- Sweeden Stage: in which land is cleared for cultivation (normally by fire) and then left to regenerate after a few years.
- Young open-canopy stage: in which the crop consists mainly of young trees that are not mature enough to produce latex.
- Productive closed-canopy stage: in which trees are mature enough to produce latex
- Fully matured closed-canopy stage

The maturity stages of para-rubber trees can be determined using the NDVI index as for the two previous types of crops (**Table 5**). Based on the experimental observation of Chen et al. [31], relation linking the age of para-rubber trees to the value of the NDVI index can be expressed by **Equation (6)**.

$$NDVI = 0.1534 * \ln(x) + 0.31 \quad (6)$$

Where x is the para-rubber tree age. Unfortunately, due to a lack of data, the production of para-rubber could not be estimated.

Table 5. Para-rubber per age [31].

States	Swidden	Young	Productive	Fully-Mature
Age (years)	0-3	4-7	7-25	>25
NDVI	0-0.479	0.524-0.610	0.610-0.805	>0.805

3.8. CNN Model

CNNs have demonstrated superior efficiency compared to traditional machine learning methods in similar tasks [14, 16], justifying their selection for this case study. Three distinct CNN models were developed, one per class (**Table 1**). The use of independent CNN models demonstrated flexibility by allowing for the easier addition of new classes compared to a single CNN model that predicts all classes simultaneously. Moreover, this approach reduces computational requirements and costs [25, 32, 36–39]. Each model consists of 'N' convolutional layers (Conv_ layer N) followed by two dense layers and a dropout layer for regularization (**Figure 3**). All layers employ the ReLU (Rectified Linear Unit) activation function to introduce non-linearity while mitigating vanishing gradient issues. A pooling rate of 0.4 was used, and a learning rate of 0.0001 was applied to enhance accuracy and reduce validation loss. The input image size was 100 × 100 × 3 (**Figure 2**), and a 3 × 3 kernel size was used. To further improve model generalization, classic data augmentation techniques were applied. These included random horizontal and vertical flipping, rotation (up to 20°), zooming (up to 10%), and brightness adjustments (within a 0.1–0.2 range). Such augmentations help simulate variations in real-world conditions while preventing overfitting. For each model, several configurations were tested, and the best one was retained at the end, resulting in a batch size of 1500 for rice, 512 for palm and 1024 for rubber (**Table 6**). A callback of 30 epochs has been used to avoid overfitting.

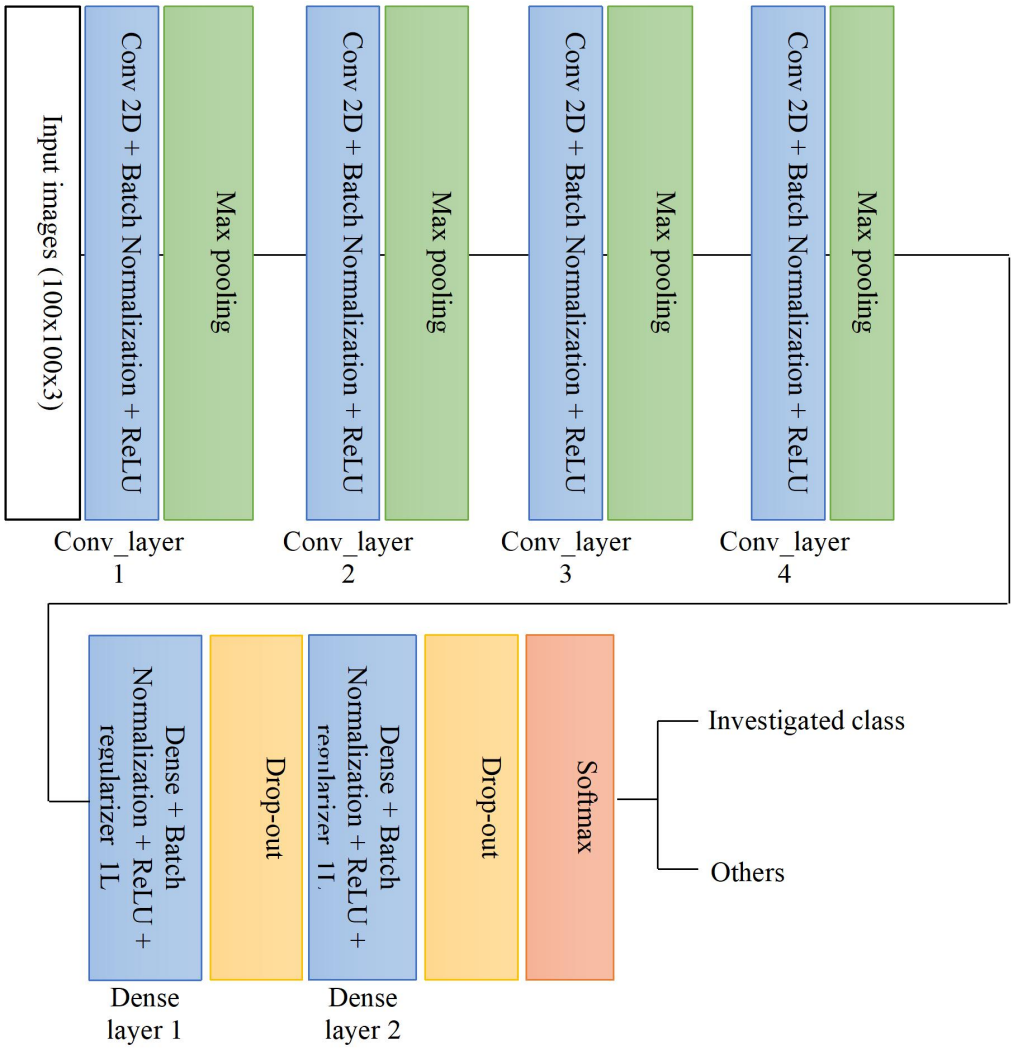

Figure 3. Flow chart of the Convolutional Neural Network architecture.

Table 6. Description of layers and batch size for each CNN model.

Layers \ CNN Model	Rice CNN	Palm CNN	Rubber CNN
Number of Convolutional layers	3	4	3
Number of neurons per Convolutional layer	8	5	16
Number of neurons per Dense layer	8	5	16
Batch size	1500	512	1024

4. Results

4.1. CNN Model Validation

The confusion matrix provides a comprehensive breakdown of the CNN model's performance, highlighting variations in class-specific accuracy[49] (Figure 4). For the Rice class, the model achieved a recall of 92%, correctly identifying 92 out of 100 instances, while misclassifying 8 as Others. The Others category for Rice demonstrated a recall of 91%, with 9 misclassifications. Precision for Rice stood at 92%, and for Others, it was 90%. Similarly, the Palm class exhibited the highest accuracy at 97%, with only 3 misclassifications, while the "Others" category for Palm achieved a recall of 95%. The precision for Palm was 92%, and for Others, it reached 95%. These metrics underscore the model's robust performance, particularly for the Palm class, while also revealing areas for potential improvement in the classification of Rice and Other categories.

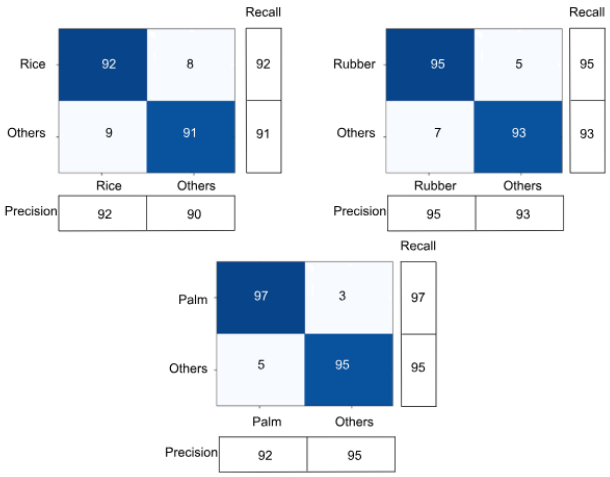

Figure 4. Confusion matrix of the 3 CNN models.

4.2. Land Cover

A representative 500 m² agricultural area in Thailand (**Figure 5a**) was classified using the proposed methodology (**Figure 5b**). The investigated area features a diverse landscape, including rice paddies, oil palm plantations, rubber tree plantations, and other agricultural land cover types, such as bare soil, forests, and water tanks. The palm class demonstrated strong predictive performance, except for newly replanted fields, which were not detected, resulting in false negatives. For the rubber class, the model successfully identified all rubber tree plantations. However, some false positives occurred in eucalyptus plantations due to their similar visual patterns and coloration to young rubber trees. Regarding the rice class model, while it detected all rice paddies, it also misclassified some bareland areas as rice fields due to their similar spectral characteristics in the imagery.

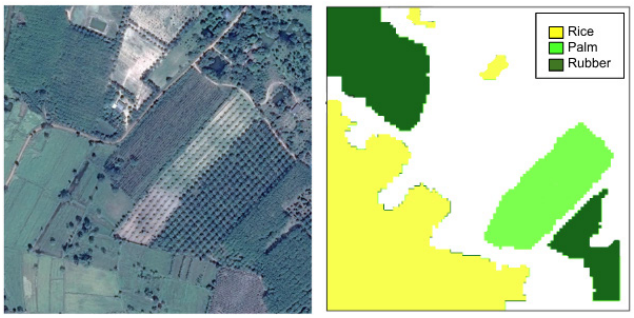

Figure 5. Investigated satellite image of 500 m² area and the associated CNN models prediction.

4.3. Diagnostic

The NDVI is computed from the reflectance values in the Red and NIR spectral bands [**Equation (1)**], generating an index map that highlights vegetation distribution (**Figure 1d**). A statistical analysis of index values across all sampling points (**Figure 1e**) reveals the spatial variability in vegetation vigor, enabling quantitative comparisons between different land cover classes. The NDVI distributions for each classified field were systematically analyzed (**Figure 6**). All fields in this study were assigned unique CP identification codes. Palm plantations exhibited consistent spectral characteristics, showing an average NDVI value of 0.7 with a standard deviation of 0.06. Integration with external validation data (**Table 4**) confirmed these values correspond to palm fields aged 3-4 years. Four distinct rice fields were identified through their characteristic NDVI signatures (**Figure 6**). The first field exhibited a pronounced bimodal distribution, characterised by a relatively low mean NDVI of 0.27 and high variability (SD = 0.15). The second field showed more concentrated reflectance values, averaging 0.46 with a tighter distribution (SD = 0.06). Field three presented a skewed distribution pattern (mean = 0.43, SD = 0.17), while field four exhibited a bimodal, skewed distribution (mean = 0.52, SD = 0.10). When cross-referenced with the agricultural database (**Table 3**), these patterns enabled age estimation, though the growth stages of fields two and three remained indeterminate due to overlapping spectral characteristics. The three rubber fields demonstrated homogeneous NDVI distributions, with mean values of 0.54, 0.64, and 0.67, respectively, and standard deviations below 0.1 in all cases. This spectral consistency facilitated reliable age determination, using Table 3 and **Equations (3)** and **(6)**, mirroring the diagnostic capability shown for palm and rice fields. All analytical results were compiled into a comprehensive summary (**Table 7**) for administrative use, presenting the complete inventory of classified fields with their respective growth stages, surface area measurements, and age determinations. This aggregated dataset provides authorities with quantitative metrics for agricultural monitoring and decision-making.

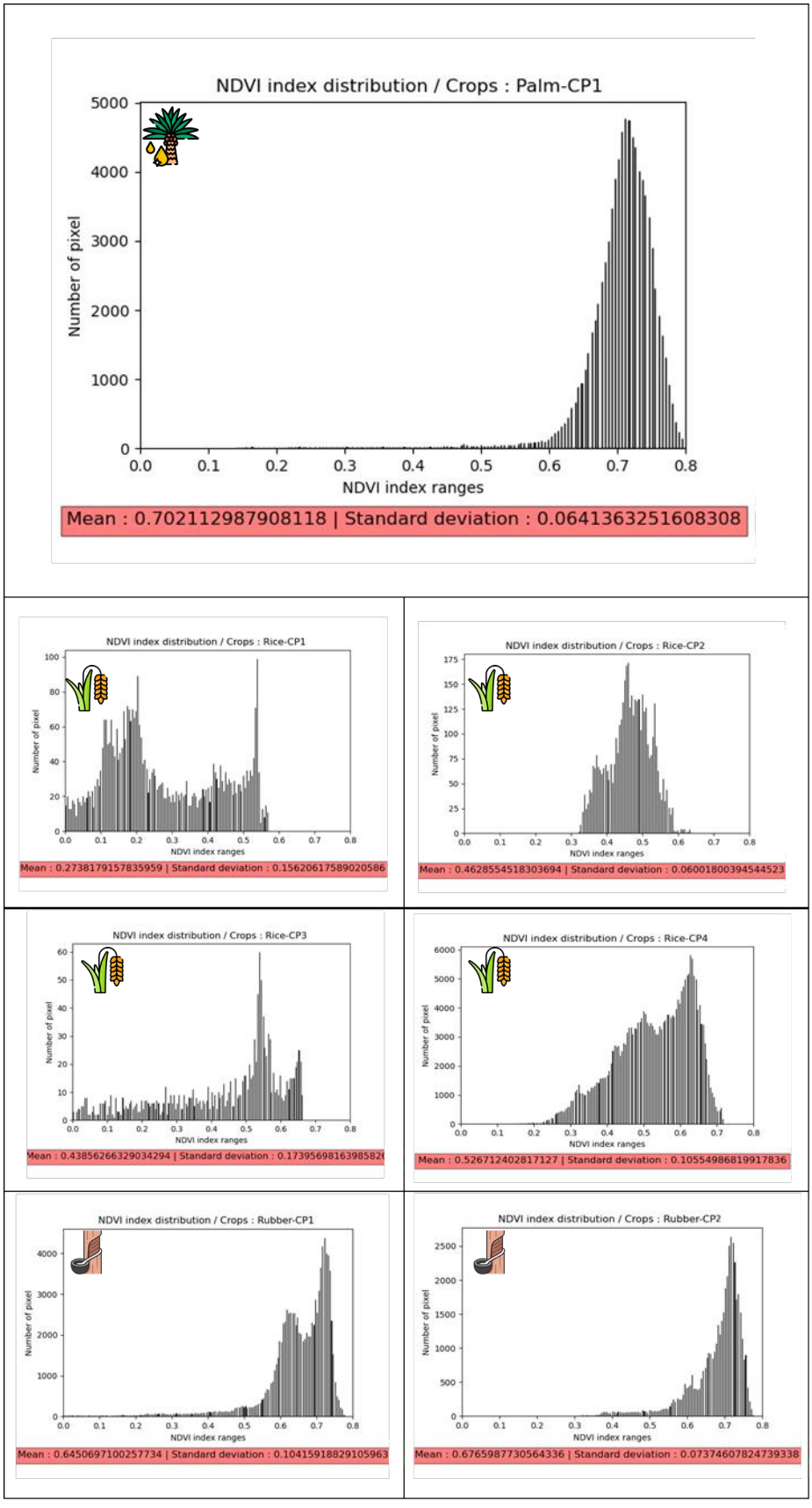

Figure 6. NDVI distribution of the different classified clusters.

Table 7. Assembled data of the 500 m² region.

Crop-ID	Class	NDVI Mean	Standard Deviation NDVI	Sub-Class (State)	Surface [ha]	Average Production
Palm-CP1	Palm	0.702	0.064	9- 14 years old	2.16	37,632 kg / 6 months
Rice-CP1	Rice	0.274	0.156	3-4 weeks	0.11	253 kg per cycle
Rice-CP2	Rice	0.463	0.060	6-8 weeks or 13-16 weeks	0.11	253 kg per cycle
Rice-CP3	Rice	0.439	0.174	4-6 weeks or more than 16 weeks	0.03	69 kg per cycle
Rice-CP4	Rice	0.527	0.106	8-13 weeks	5.92	13,616 kg per cycle
Rubber-CP1	Rubber	0.645	0.104	4 years old	2.55	/
Rubber-CP2	Rubber	0.545	0.073	3 years old	1.46	/
Rubber-CP3	Rubber	0.676	0.073	5 years old	1.11	/

5. Discussion

5.1. Application

The method demonstrates its ability to provide information and can be applied over a large area of 100 km^2 (**Figure 7**). The total surface of palm, rice and rubber classified is 4.48 km^2, 6.22 km^2 and 9.35 km^2, respectively. The gathered data detailing each state is given in **Figure 8,** and the calculated production of rice and palm is 91,448 kg per cycle and 5,334 tons/6 months of rice and palm, respectively.

Figure 7. Investigated satellite image of a 100 km^2 area.

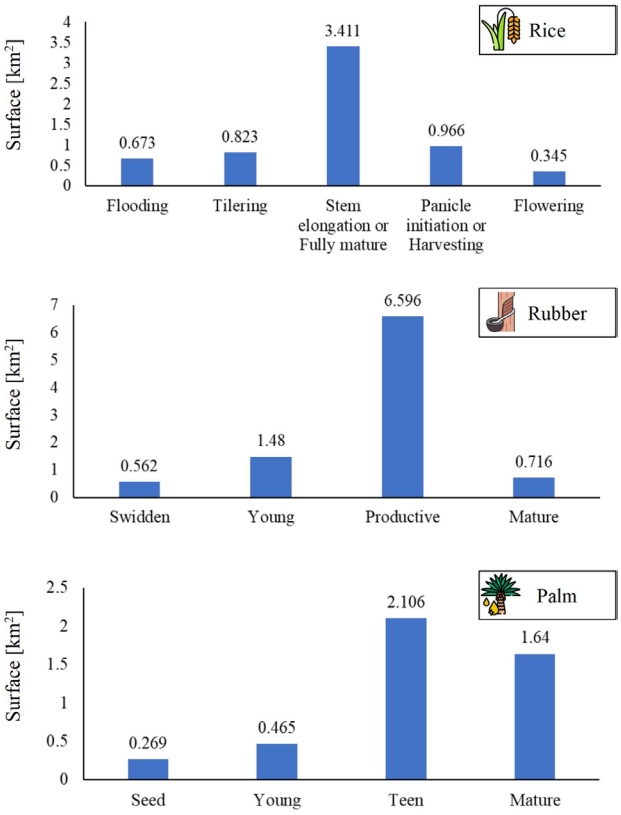

Figure 8. Total surface for each crop and different states for the 100 km^2 region.

5.2. Comparison with Reference Measures

Results obtained from the large area (**Table 8**) can be compared with those obtained using the accurate hand measurements performed by GISTDA, which are used as reference (**Table 8**). Error is defined as:

$$\text{Error} = \frac{CNN\ model - measures}{measures} \times 100 \quad (7)$$

It can be observed that the error between the reference measurements and CNN predictions is -12% for the palm and about -20% for the other two classes. For each class, the CNN model underpredicts the reference measurements. Palm shows the lowest difference due to the highest accuracy of the CNN model (**Figure 4**). The other two classes present higher differences due to the difficulty in classifying the edge of the crops (**Figure 9**), as explained by Lu et al. [50].

A deeper analysis reveals that several factors contribute to these misclassifications. One of the primary causes stems from issues with edge detection. Crop boundaries often present mixed spectral signals, especially when adjacent fields are composed of different vegetation types or when transitional zones (e.g., between rice paddies and bare land) are encountered. As a result, the CNN models sometimes confuse adjacent classes, leading to a degradation of boundary precision. Additionally, spectral similarities between certain classes further complicate the classification task. For example, young rubber plantations can present visual and spectral features similar to eucalyptus plantations, both exhibiting comparable canopy textures and color tones in the satellite images. Similarly, bare lands with low vegetation cover can be misclassified as early-stage rice fields, given their low NDVI values and similar reflectance patterns in the RGB bands used. These factors collectively contribute to the observed errors, particularly for rice and rubber classes, which showed higher discrepancies compared to palm classification.

Table 8. Comparison between the reference area and the CNN prediction.

	Rice	Rubber	Palm
Reference surface [km²]	8.05	11.92	5.09
CNN surface prediction [km²]	6.22	9.35	4.48
Error [**Equation (7)**]	-22%	-21%	-12%

5.3. Benefits

The developed tool offers valuable opportunities to inform policy decisions at both local and national levels. By providing accurate land cover classifications and detailed diagnostics on crop types, age, and estimated production, authorities such as the Ministry of Agriculture can better allocate subsidies to farmers based on actual crop types and conditions, promoting fairness and transparency. Additionally, insights into the spatial distribution and maturity of agricultural lands can support strategic land use planning, including zoning for crop rotation, the identification of ageing plantations requiring renewal, and prioritization of agricultural investments. Moreover, early identification of underperforming fields through NDVI-based diagnostics can help guide targeted interventions and resource allocation, thereby enhancing overall agricultural productivity. Therefore, integrating the proposed CNN-based land cover tool into existing agricultural management frameworks could significantly strengthen data-driven decision-making for sustainable agricultural development in Thailand.

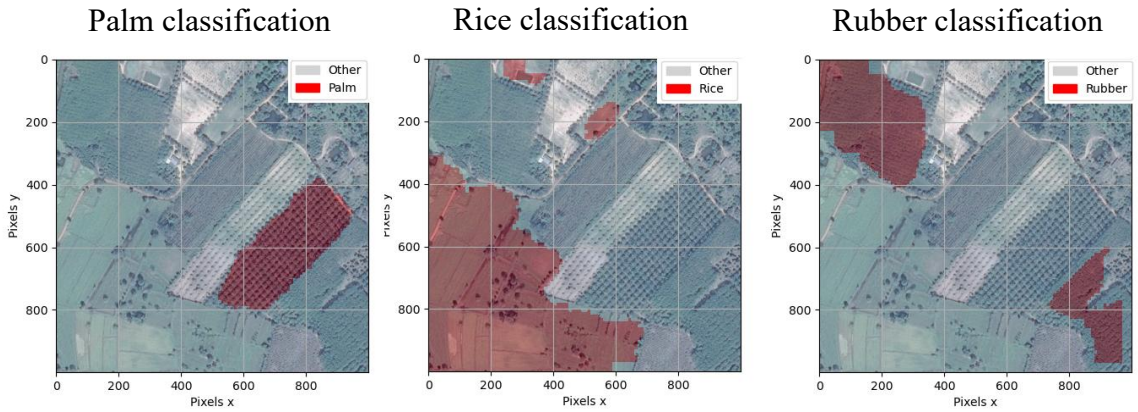

Figure 9. Edge classification of palm, rice and rubber of the 500m^2 area.

5.4. Limitations

CNN models have been trained using images of the two different studied areas (**Figure 2**). Although interesting results have been obtained in terms of classification, the applicability of the CNN models could be restricted to these specific areas, and their accuracy in other regions remains uncertain. Hence, it is possible that the suggested CNN models might not be efficient in generating accurate labels for other regions. To enhance generalizability, it is recommended that more diverse datasets be incorporated, including images from different geographical regions, crop types, and temporal variations. Additionally, transfer learning approaches could be employed, allowing pre-trained models to be fine-tuned with a smaller amount of new data from different regions, thereby improving adaptability while reducing the annotation burden [51]. A larger dataset should be used to represent the diversity of the three better investigated crops presented in Thailand across different periods. However, creating such a large dataset will require the annotation of a large number of tiles to achieve high accuracy, which is a challenging task. To improve the prediction of crop edges, post-processing techniques can be applied as proposed by Dong et al. [52]. A Fully Connected Conditional Random Field (FC-CRF) has been employed to refine the segmentation results, yielding an improvement in overall accuracy of 1.48% a 1.4% increase in the mean Intersection-over-Union (IoU).

6. Conclusion

Precision agriculture serves as a valuable tool for enhancing production management. This study successfully classified and diagnosed three key crop types in Thailand—rice, rubber, and palm—using dedicated CNN models. Each CNN model was trained on a dataset comprising 200,000 tiles (100 × 100 pixels at 0.5 m/pixel resolution), achieving classification accuracies exceeding 92%. Following model predictions, post-processing techniques were applied to generate comprehensive land cover maps. Subsequent diagnostic analysis utilizing NDVI indices enabled crop age determination and production estimation.

Validation across a 100 km² study area revealed prediction differences of 12%, 21%, and 22% for palm, rubber, and rice, respectively, when compared to ground reference measurements. These results demonstrate the effectiveness of the method in crop classification, status identification, and production estimation. Current efforts focus on enhancing existing class datasets, particularly for crop edge detection, while expanding the framework to incorporate additional crops, such as cassava and eucalyptus. Future work will explore supplementary vegetation indices, including the SAVI, to further improve diagnostic capabilities.

Author Contributions

Y.L: Coding, Analysis, Data curation; L.M: Methodology, Supervision, Data, Resources, Writing original paper and reviewing.

Funding

No funding to declare.

Informed Consent Statement

Not applicable.

Data Availability Statement

Data are available on request.

Acknowledgments

The authors would like to thank the Geo-Informatics and Space Technology Development Agency (GISTDA) for its operational and other related support in facilitating the progress of the research.

Conflict of Interest

The Authors declare that there is no conflict of interest.

References

[1] UN, 2023. Global Issues Population. Available from: https://www.un.org/en/global-issues/population (cited 10 August 2023).

[2] Griffiths, P., Nendel, C., Hostert, P., 2019. Intra-annual reflectance composites from Sentinel-2 and Landsat for national-scale crop and land cover mapping. Remote Sensing of Environment. 220, 135–151. DOI: https://doi.org/10.1016/j.rse.2018.10.031

[3] Palazzi, V., Bonafoni, S., Alimenti, F., et al., 2019. Feeding the world with microwaves: how remote and wireless sensing can help precision agriculture. IEEE Microwave. 20(12), 72–86. DOI: https://doi.org/10.1109/MMM.2019.2941618

[4] Yu, L., Gong, P., Clinton, N., et al., 2014. Meta-discoveries from a synthesis of satellite-based land-cover mapping research. International Journal of Remote Sensing. 35(13), 4573–4588. DOI: https://doi.org/10.1080/01431161.2014.930206

[5] Saah, D., Tenneson, K., Poortinga, A., et al., 2019. Land cover mapping in data scarce environments: challenges and opportunities. Frontiers in Environmental Science. 7, 150. DOI: https://doi.org/10.3389/fenvs.2019.00150

[6] Som-ard, J., Immitzer, M., Vuolo, F., et al., 2022. Mapping of crop types in 1989, 1999, 2009 and 2019 to assess major land cover trends of the Udon Thani Province, Thailand. Computers and Electronics in Agriculture. 198, 107083. DOI: https://doi.org/10.1016/j.compag.2022.107083

[7] Dorber, M., Verones, F., Nakaoka, M., et al., 2020. Can we locate shrimp aquaculture areas from space? – A case study for Thailand. Remote Sensing Applications: Society and Environment. 20, 100416. DOI: https://doi.org/10.1016/j.rsase.2020.100416

[8] Chirachawala, C., Shrestha, S., Babel, M., et al., 2019. Evaluation of global land use/land cover products for hydrologic simulation in the Upper Yom River Basin, Thailand. Science of the Total Environment. 708, 135148. DOI: https://doi.org/10.1016/j.scitotenv.2019.135148

[9] Bouvet, A., Le Toan, T., Lam-Dai, L., et al.., 2018. An above-ground biomass map of African savannahs and woodlands at 25 m resolution derived from ALOS PALSAR. Remote Sensing of Environment. 206, 156–173. DOI: https://doi.org/10.1016/j.rse.2017.12.030

[10] Johnson, D.M., 2019. Using the Landsat archive to map crop cover history across the United States. Remote Sensing of Environment. 232, 111286. DOI: https://doi.org/10.1016/j.rse.2019.111286

[11] Singha, M., Rahman, M., Huete, A., et al., 2020. Identifying floods and flood-affected paddy rice fields in Bangladesh based on Sentinel-1 imagery and Google Earth Engine. ISPRS Journal of Photogrammetry and Remote Sensing. 166, 278–293. DOI: https://doi.org/10.1016/j.isprsjprs.2020.06.011

[12] Yang, H., Pan, B., Li, N., et al., 2021. A systematic method for spatio-temporal phenology estimation of paddy rice using time series Sentinel-1 images. Remote Sensing of Environment. 259, 112394. DOI: https://doi.org/10.1016/j.rse.2021.112394

[13] Zhu, A.X., Zhao, F.H., Pan, H.B., et al., 2021. Mapping rice paddy distribution using remote sensing by coupling deep learning with phenological characteristics. Remote Sensing. 13(7), 71360. DOI: https://doi.org/10.3390/rs13071360

[14] Watanabe, F., Tani, H., Wang, X., et al., 2020. Inland water's trophic status classification based on machine learning and remote sensing data. Remote Sensing Applications: Society and Environment. 19, 100326. DOI: https://doi.org/10.1016/j.rsase.2020.100326.

[15] Yoo, C., Han, D., Im, J., et al., 2019. Comparison between convolutional neural networks and random forest for local climate zone classification in mega urban areas using Landsat images. ISPRS Journal of Photogrammetry and Remote Sensing. 157, 155–170. DOI: https://doi.org/10.1016/j.isprsjprs.2019.09.009

[16] Panahi, M., Sadhasivam, N., Pourghasemi, H.R., et al., 2020. Spatial prediction of groundwater potential mapping based on convolutional neural network (CNN) and support vector regression (SVR). Journal of Hydrology. 588, 125033. DOI: https://doi.org/10.1016/j.jhydrol.2020.125033

[17] Li, W., Chen, C., Zhang, M., et al., 2019. Data augmentation for hyperspectral image classification with deep CNN. IEEE Geoscience and Remote Sensing Letters. 16(4), 593–597. DOI: https://doi.org/10.1109/LGRS.2018.2878773

[18] Guo, Y., Liu, Y., Wang, L., et al., 2020. Plant disease identification based on deep learning algorithm in smart farming. Discrete Dynamics in Nature and Society. 2020(1), 2479172. DOI: https://doi.org/10.1155/2020/2479172

[19] Kanda, P.S., Xia, K., Sanusi, O.H., 2021. A deep learning-based recognition technique for plant leaf classification. IEEE Access. 9, 162590–162613. DOI: https://doi.org/10.1109/ACCESS.2021.3131726

[20] Olsen, A., Konovalov, D.A., Philippa, B., et al., 2019. DeepWeeds: a multiclass weed species image dataset for deep learning. Scientific Reports. 9(1), 3843. DOI: https://doi.org/10.1038/s41598-018-38343-3

[21] Kipli, K., Dahlan, M.R., Rahman, A.A., et al., 2023. Deep learning applications for oil palm tree detection and counting. Smart Agricultural Technology. 5, 100241. DOI: https://doi.org/10.1016/j.atech.2023.100241

[22] Thorp, K.R., Drajat, D., 2021. Deep machine learning with Sentinel satellite data to map paddy rice production stages across West Java, Indonesia. Remote Sensing of Environment. 265, 112679. DOI: https://doi.org/10.1016/j.rse.2021.112679

[23] Yan, C., Li, Z., Zhang, Z., et al., 2023. High-resolution mapping of paddy rice fields from unmanned airborne vehicle images using enhanced-TransUnet. Computers and Electronics in Agriculture. 210, 107867. DOI: https://doi.org/10.1016/j.compag.2023.107867

[24] Xia, L., Zhang, Y., Liu, S., et al., 2022. A full resolution deep learning network for paddy rice mapping

using Landsat data. ISPRS Journal of Photogrammetry and Remote Sensing. 194, 91–107. DOI: https://doi.org/10.1016/j.isprsjprs.2022.10.005

[25] Mentet, M., Hongkarnjanakul, N., Schwob, C., et al., 2022. Method to apply and visualize physical models associated to a land cover performed by CNN: a case study of vegetation and water cooling effect in Bangkok, Thailand. Remote Sensing Applications: Society and Environment. 28, 100856. DOI: https://doi.org/10.1016/j.rsase.2022.100856

[26] Jinru, X., Su, B., 2017. Significant remote sensing vegetation indices: a review of developments and applications. Journal of Sensors. 2017, 1–17. DOI: https://doi.org/10.1155/2017/1353691

[27] Huete, A.R., 2004. 11 - Remote sensing for environmental monitoring. In: Artiola, J.F., Pepper, I.L., Brusseau, M.L. (eds.). Environmental Monitoring and Characterization. Academic Press: Burlington, MA, USA. pp. 183–206. DOI: https://doi.org/10.1016/B978-012064477-3/50013-8

[28] Bhandari, A., Kumar, A., Singh, G.K., 2012. Feature extraction using normalized difference vegetation index (NDVI): a case study of Jabalpur City. Procedia Technology. 6, 612–621. DOI: https://doi.org/10.1016/j.protcy.2012.10.074

[29] Rahmanida, Y., Shidiq, I.P.A., Rokhmatuloh, et al., 2021. Spatial distribution of rice productivity utilizes Sentinel-2A and NDVI algorithm in Nagrak Sub-district, Sukabumi Regency. Proceedings of The International Conference on Environment, Sustainability Issues, and Community Development; October 21, 2020; Semarang, Indonesia. pp. 1–6. DOI: https://doi.org/10.1088/1755-1315/623/1/012037

[30] Marzukhi, F., Elahami, A., Bohari, S., 2016. Detecting nutrients deficiencies of oil palm trees using remotely sensed data. Proceedings of The 8th IGRSM International Conference and Exhibition on Geospatial & Remote Sensing (IGRSM 2016); April 13–14, 2016; Kuala Lumpur, Malaysia. pp. 1–11. DOI: https://doi.org/10.1088/1755-1315/37/1/012040

[31] Chen, G., Thill, J.C., Anantsuksomsri, S., et al., 2018. Stand age estimation of rubber (*Hevea brasiliensis*) plantations using an integrated pixel- and object-based tree growth model and annual Landsat time series. ISPRS Journal of Photogrammetry and Remote Sensing. 144, 94–104. DOI: https://doi.org/10.1016/j.isprsjprs.2018.07.003

[32] Fitton, D., Laurens, E., Hongkarnjanakul, N., et al., 2022. Land cover classification through convolutional neural network model assembly: a case study of a local rural area in Thailand. Remote Sensing Applications: Society and Environment. 26, 100740. DOI: https://doi.org/10.1016/j.rsase.2022.100740

[33] Sangbuapuan, N., 2013. Strengthening the rice production in Thailand through Community Rice Centers (CRCs) using ICT policies. Proceedings of The 2013 IEEE/ACIS 12th International Conference on Computer and Information Science (ICIS); June 16–20, 2013; Niigata, Japan. pp. 553–558. DOI: https://doi.org/10.1109/ICIS.2013.6607899

[34] Ritchie, H., Roser, M., 2021. Forests and deforestation. Our World in Data. Available from: https://ourworldindata.org/palm-oil (cited 7 September 2023).

[35] Statista, 2023. Statista – The Statistics Portal. Available from: https://www.statista.com/ (cited 25 August 2023).

[36] Chermprayong, P., Hongkarnjanakul, N., Rouquette, D., et al., 2021. Convolutional neural network for Thailand's Eastern Economic Corridor (EEC) land cover classification using overlapping process on satellite images. Remote Sensing Applications: Society and Environment. 23, 100543. DOI: https://doi.org/10.1016/j.rsase.2021.100543

[37] Emparanza, P.R., Hongkarnjanakul, N., Rouquette, D., et al., 2020. Land cover classification in Thailand's Eastern Economic Corridor (EEC) using convolutional neural network on satellite images. Remote Sensing Applications: Society and Environment. 20, 100394. DOI: https://doi.org/10.1016/j.rsase.2020.100394

[38] Sentagne, T., Zerbola, M., Garcia, M., et al., 2023. Method to map human and infrastructure vulnerability using CNN land cover: case study of floating tank explosion at petrochemical plants of Laem Chabang, Thailand. Journal of Loss Prevention in the Process Industries. 83, 105057. DOI: https://doi.org/10.1016/j.jlp.2023.105057

[39] Marty, B., Gaudin, R., Piperno, T., et al., 2024. Methodology to classify high voltage transmission poles using CNN approach from satellite images for safety public regulation application: Study case of rural area in Thailand. Systems and Soft Computing. 6, 200080. DOI: https://doi.org/10.1016/j.sasc.2024.200080

[40] Xie, J., Hu, K., Guo, Y., et al., 2021. On loss functions and CNNs for improved bioacoustic signal classification. Ecological Informatics. 64, 101331. DOI: https://doi.org/10.1016/j.ecoinf.2021.101331

[41] Hasan, F., Ali, M., Rahman, M., 2011. A digital approach of satellite image processing for retrieving surface parameters. International Journal of Engineering Research and Applications. 1, 1242–1246.

[42] Peters, A.J., Walter-Shea, E., Ji, L., et al., 2002. Drought monitoring with NDVI-based Standardized Vegetation Index. Photogrammetric Engineering and Remote Sensing. 68, 71–75.

[43] Supriatna, S., Rokhmatuloh, R., Wibowo, A., et al., 2020. Rice productivity estimation by Sentinel-2A imagery in Karawang Regency, West Java, Indonesia. International Journal of GEOMATE. 19, 205–210.

DOI: https://doi.org/10.21660/2020.72.5622

[44] Dipa, P., 2012. data time series NDVI-SPOT VEGETATION for rice plants[In Indonesian], [Undergraduate Thesis]. Bogor, Indonesia: Bogor Agricultural University (IPB). pp. 1–31.

[45] Orawan, S., 2023. Rice economy in Northeast Thailand: current status and challenges. FFTC Agricultural Policy Platform (FFTC-AP). Available from: https://ap.fftc.org.tw/article/1863 (cited 7 September 2023).

[46] Fitrianto, A., Tokimatsu, K., Wijaya, M.S., 2017. Estimation the amount of oil palm trees production using remote sensing technique. Proceedings of The 5th Geoinformation Science Symposium 2017 (GSS 2017); September 27–28, 2017, Yogyakarta, Indonesia. pp. 1–7. DOI: https://doi.org/10.1088/1755-1315/98/1/012016

[47] Chemura, A., van Duren, I., van Leeuwen, L.M., 2015. Determination of the age of oil palm from crown projection area detected from WorldView-2 multispectral remote sensing data: the case of Ejisu-Juaben district, Ghana. ISPRS Journal of Photogrammetry and Remote Sensing. 100, 118–127. DOI: https://doi.org/10.1016/j.isprsjprs.2014.07.013

[48] Xu, J., Yi, Z.F., 2015. Socially Constructed Rubber Plantations in the Swidden Landscape of Southwest China. In: Fox, J., Castella, J.C., Ziegler, A.D. (eds.). Shifting Cultivation and Environmental Change. Routledge: London, UK. pp. 794–810.

[49] Olson, D., Delen, D., 2008. Advanced Data Mining Techniques. Springer: Berlin, Germany. pp. 1–180. DOI: https://doi.org/10.1007/978-3-540-76917-0

[50] Lu, R., Zhang, Y., Huang, Q., et al., 2024. A refined edge-aware convolutional neural networks for agricultural parcel delineation. International Journal of Applied Earth Observation and Geoinformation. 133, 104084.

[51] Liu, Z., Li, J., Ashraf, M., et al., 2024. Remote sensing-enhanced transfer learning approach for agricultural damage and change detection: a deep learning perspective. Big Data Research. 36, 100449.

[52] Dong, R., Li, J., Zhang, Y., et al., 2020. Oil palm plantation mapping from high-resolution remote sensing images using deep learning. International Journal of Remote Sensing. 41(5), 2022–2046. DOI: https://doi.org/10.1080/01431161.2019.1681604